The EPIGENOME Network of Excellence

Tracking individual chromosomes with integrated arrays of *Lac*^{op} sites and GFP-*Lac*^{i} repressor (PROT15)

Frank Neumann, Angela Taddei & Susan Gasser
The Friedrich Miescher Institute for Biomedical Research
Maulbeerstrasse 66
CH-4058 Basel, Switzerland

Email feedback to:
fneumann@rockefeller.edu

Last reviewed: 02 Nov 2005 by Julio Vazquez, Fred Hutchinson Cancer Research Center, Seattle

Introduction

The visualisation of specific DNA sequences in living cells, achieved through the integration of *lac* operator arrays (*lac*^{op}) and expression of a GFP-*lac*
repressor fusion, has provided new tools to examine how the nucleus is organised and how basic events like sister chromatid separation occur (Straight *et al*. 1996; Belmont 2001). In contrast to other methods, such as fluorescence *in situ* hybridisation, the *lac*^{op}/GFP-*lac* repressor (GFP-*lac*^{i}) technique is non-invasive, and therefore interferes minimally with nuclear structure and function. In addition, it facilitates analysis of the rapid dynamics of specific DNA loci (Gasser, 2002). Although this technique has been adapted to organisms from bacteria to man, the ease with which GFP fusions can be targeted to specific chromosomal sites depends on the organism's ability to carry out homologous recombination. This process is very efficient in budding yeast, allowing pairs of chromosomal loci to be analysed at the same time through the use of two bacterial repressors (lac^{i} and *tetR*) fused to different GFP variant. Given the relatively advanced state of the art in budding yeast, we present protocols optimised for this organism. These provide a starting point for adapting multi-locus tagging to other species. Moreover, the techniques described here for the quantitative analyses of locus dynamics are universally applicable.

Procedure

Preparations

Plasmids and Strains

Yeast transformation and growth are as described (Guthrie *et al*. 1991). The *lac*^{op}/ GFP-*lac*^{i} system for site recognition exploits the high affinity and specificity of the bacterial *lac* repressor for its recognition sequence (*lac*^{op}). All procedures are performed analogously for the *tetR*/*tet*^{op} system (Michaelis *et al*. 1997).

1. Plasmids or integrations of repetitive arrays are difficult to propagate in both bacteria and yeast, due to recombination induced excision events. To avoid this, bacteria should be grown at 30°C in a recombination deficient strain (STBL2 (Invitrogen Life Technologies) or SURE (Stratagene));
2. Integrate a copy of *lac*
repressor fused in frame to sequences encoding the S65T V163A, S175G derivative of GFP and a Nuclear Localisation Signal, e.g. pAFS144 into the yeast strain. This red-shifted GFP-derivative has a higher emission intensity and longer fluorescence time than natural GFP (Straight *et al*. 1998). The lac^{i} later helps to stabilise the *lac*^{op} array in yeast.;
3. Insert a multimerised *lac*^{op}
array (usually 256 copies or ~10 kb) into the chromosome, by standard transformation using a linearised construct that integrates by homologous recombination. Integration is directed to a genomic locus by a unique cleavage within a PCR generated genomic sequence >200bp inserted into the host plasmid (e.g. pAFS52 integration is selected by growth on SD-trp; Straight *et al*. 1996; Heun *et al*. 2001a; Hediger *et al*. 2002). In yeast as few as 24 contiguous *lac*^{op} sites can be readily detected;
4. Check the proper insertion by standard colony-PCR and/or Southern blotting (Guthrie *et al*. 1991). Binding of lac^{i}-GFP to

the *lac*^{op}
array results in a bright focal spot, readily detected by fluorescence microscopy within the nucleoplasm. Confirmed transformants with bright signals should be frozen and stored immediately as individual colony isolates. When strains are recovered from frozen stocks, they should be grown on selective medium, to avoid further excision events. Note: Other GFP-fusions, optimised forms of CFP or YFP (or ECFP and EYFP), have also been successfully used in yeast (Lisby *et al*. 2003). The *lac*
repressor used is also modified to prevent tetramerisation, thus minimising artefactual higher order interactions between *lac*^{op} sites (Straight *et al*. 1996);

5. Double tagging: If the position or mobility of two genomic loci are to be compared, one should avoid tagging both with the same repeats. It has been shown that identical arrays can undergo a pairing event that, at least in the case of the *tet* system, depends on the expression of the repressor (*tetR*; Fuchs *et al*. 2002). By using *tet*^{op} for one site, and *lac*^{op} for the second, the risk of spurious pairing is eliminated. Useful pairs of GFP derivatives are CFP and YFP, or GFP and the new monomeric mRFP (Campbell *et al*. 2002);
6. In contrast to the lac^{i} GFP fusion (Figures 1A and 1B), the *tetR*-GFP gives a high and generally diffuse nucleoplasmic background in yeast, both in the presence and absence of *tet*^{op} repeats (Figures 1C and 1D);
7. Dynamics: If movement analysis is to be pursued it is important to differentiate the movement of the nucleus itself or that induced by mechanical vibrations, from the dynamics of the chromosome. Nuclear movement can be subtracted from that of a specifically tagged site by any of the following three methods:
    a. Visualisation of the nuclear envelope with Nup49-GFP (Belgareh *et al*. 1997; Heun *et al*. 2001a). In this case the nuclear centre can be interpolated from the oval or circular pore signal in an automated fashion by software such as ImageJ or Metamorph (Figures 1A and 1B). The DNA locus position is then determined relative to the nuclear centre for each frame.
    b. Diffuse nucleoplasmic signal of *tetR*-GFP (Figures 1C and 1D). The centre of the nucleus is defined by interpolation frame-by-frame and locus movement is calculated relative to this;
    c. By comparing the motion of two tagged loci, one can calculate average movement without concern for nuclear drift. The fact that both loci are moving has to be taken into account for movement quantitation (see below).

Growth and cell preparation

1. All yeast strains to be analysed should be cultured identically and preferably to an early exponential phase of growth (< $0.5x10^{7}$
cells/ml) in synthetic or YPD medium, starting from a fresh overnight culture. Wash cells once before observation, to avoid YPD autofluorescence. We recommend two mounting techniques for living cell visualisation;
2. A. SD-Agarose-filled slides (Figure 2A): Cells are immobilised between an agarose patch on a depression slide and a coverslip, to avoid flattening or distortion of the yeast by coverslip pressure on a normal glass slide. Cells sealed in this way are in a closed environment in which the depletion of O_2 and production of CO_2 bubbles can influence growth and impair visualization. Optimally this technique is used for imaging periods limited to < 60 minutes;
    a. Melt an aliquot of SD/agarose at 95°C until the agarose has completely melted, but not longer;
    b. Vortex briefly and transfer 150µl into the well of a depression slide that is preheated either by a heating block or by passage through the flame of a Bunsen burner;
    c. Immediately pass a normal microscope slide over the depression to remove excess agarose as depicted in Figure 2A;
    d. While the agarose solidifies, recover the cells from 1ml of culture by centrifugation for 1 minute at < 10000g;
    e. Resuspend the cells in ~20µl of appropriate medium;
    f. Once the agarose has solidified remove the upper slide by sliding along the depression slide surface and place ~5µl of concentrated cells on the agarose patch;
    g. Close with a coverslip, eliminate eventual air bubbles and seal with nail polish. Note: Monitor bud emergence and cell division carefully, as some brands of nailpolish contain solvents that negatively influence yeast cell physiology.

    B. Cell observation chamber (Ludin chamber, Figure 2B): The second technique uses a Ludin chamber in which cells are non-covalently attached to a coverslip by a lectin. The chamber medium-filled chamber is assembled as shown in Figure 2B. A flow of fresh medium can be applied;
    a. Coat 18mm coverslips with 10µl ConA (1mg/ml in H_2O) and let them air-dry for >20 minutes. Coated slides can be kept for weeks at room temperature;
    b. Adhere cells to the ConA-coated coverslip by sedimenting 1ml of the culture at 1 x g during 3 minutes at room temperature;
    c. Remove the excess culture and add ~1ml fresh preheated medium before closing the chamber.

Temperature control

In order to have a stable condition for microscopic observation, the temperature of the microscope and room should be carefully controlled (±2°C). Two mechanisms are standardly used. The first is to enclose the entire imaging part of the microscope in a commercially available temperature regulated box, which is commercially available (e.g. Life Imaging Services or Zeiss). A second, less precise method is to regulate the temperature of the slide through a heated stage.

Image Acquisition

General

The choice of imaging technique depends on the question being asked. To derive quantitative information on the position of a given locus relative to a fixed structure (e.g. the spindle pole body, nucleolus or nuclear envelope), three dimensional (3D) stacks and detection of different wavelengths may be necessary. An analysis of fine movement and chromatin dynamics, on the other hand, requires the rapid and extended capture of one or more fluorochromes. Bleaching of the signal is often a major limiting factor in time-lapse imaging. One should note that chromatin movement is very fast (movements > 0.5µm in less than 10 seconds, (Heun *et al*. 2001a)), making it necessary to have rapid image acquisition with a minimal interval between sequential images. To optimise the acquisition, the parameters such as image resolution, the number of z frames, intervals between frames, light intensity, and exposure time can be varied. In all cases, it is of utmost importance to minimise and monitor laser- or light-induced damage to the organism during imaging, in part by determining the time required for one division cycle in imaged and non-imaged cells:

Cell cycle determination:
As position and mobility of a chromosomal locus can vary with stages of the cell cycle, it is crucial to determine precisely what stage each imaged cell is in. This is done by monitoring bud presence, bud size, as well as the shape and position of the nucleus, as visualised by the Nup49-GFP fusion and a transmission or phase image. Figure 3 summarises the morphologies that characterise each stage of the cell cycle.

Widefield Microscopy and Deconvolution:
For the imaging of large fields of cells, best results are obtained with a widefield microscope equipped with a PIFOC, Xenon light source and monochromator that allows a broad and continuous range of incident light wavelengths, as well as rapid switching between these values. Images are acquired by a high-speed monochrome CCD camera run by a rapid imaging software, such as Metamorph. The limiting step is often the speed of signal transfer from the CCD chip to the RAM and/or hard disk of your computer.

z-stacks:
Widefield microscopy is well adapted to experiments in which a large number of cells (200-300) need to be scored, for example, when determining the subnuclear position of a given locus relative to the nuclear envelope or another tagged locus or landmark (e.g. spindle pole body or nucleolus). The reference point should optimally be tagged with a different fluorescent protein. If two loci bind the same fluorescent fusion proteins, then their intensities should be significantly different. Rapid through-focus stacks of images using the full chip capacity of the camera are taken of cells growing on agar or in a Ludin chamber (such that 20-30 individual cells are resolved per field). Optimal parameters for GFP are as follows: exposure time, 100-200 ms; z-spacing of 200nm for 18 focal planes, excitation wavelength 475nm. For dual wavelength capture, images of both wavelengths (CFP: 432nm, ~300ms;YFP: 514nm, ~150ms) must be acquired before the focal plane changes. A phase image is taken after every stack of fluorescence images. Widefield images have out-of-focus haze and deconvolution of the z-stack is often necessary to reassign blurred intensities back to their original source. Use Metamorph software, or other available deconvolution packages.

3D time-lapse:
The conditions for capturing 3D time-lapse series are as follows: 5-11 optical z slices taken every 1 to 4 minutes, z sections are 200-400 nm in depth and the exposure time is ~50ms. Using these settings up to 300 stacks of 5 sections each (1500 frames) at 1 minute intervals can be captured without affecting cell cycle progression. More rapid sampling with this system, on the other hand, leads to bleaching and potential cellular damage. Until this can be remedied by more rapid and more sensitive CCD cameras, widefield microscopy is recommended for less rapid time-lapse imaging (intervals ≥ 60 seconds) on larger fields and confocal microscopy (see below) for very rapid time-lapse imaging (intervals ≤ 2 seconds) on small regions of interest (typically one yeast nucleus).

For very long imaging times (> 1 hour), stray light should be suppressed by inserting an additional shutter. Deconvolution is performed using the Metamorph fast algorithm with 5 iterations, sigma parameter of 0.7 and a frequency of 4.

Confocal Microscopy

To follow chromatin dynamics in individual cells with rapid time-lapse microscopy, the Zeiss LSM510 scanning confocal microscope is particularly well adapted, although the laser and AOTF (acousto-optic tuneable filter) system is limited in activation wavelengths. Its positive attributes are an ability to limit scanhead motion to a minimal region of interest (ROI), rapid and well regulated scanning speeds and the possibility to adjust pinhole aperture and laser intensities to very low levels, while maintaining maximal sensitivity.

General settings:
To reduce the risk of damage by illumination, the laser transmission is kept as low as possible, and the cells are imaged as rapidly as possible within a minimal Region of Interest (ROI). Useful settings for the Zeiss LSM510 are as follows:

- Laser: Argon/2 458, 488 or 514 nm tube current 4.7 Amp. Output 25%;
- Filters: Channel 1: Lp 505 for GFP alone ; Channel 1 Lp 530, Channel 3 Bp 470-500 for YFP/CFP single track acquisition;

- Channel setting: Pinhole 1-1.2 Airy unit (corresponding to optical slice of 700-900nm); detector gain: 930-999; amplifier gain: 1-1.5; amplifier offset: 0.2V0.1V; laser transmission AOTF = 0.1-2% for GFP alone, 1-15 % for YFP and 10 50% for CFP in single track acquisition. In order to use minimal laser transmission the pinhole must be regularly aligned;
- Scan setting: speed 10 (0.88µs/pixel); 8 bits one scan direction; 4 average/Mean/Line; zoom 1.8 (pixel size: 100x100 nm);
- Imaging intervals: 1.5 seconds.

Note: If CFP and YFP signals are very weak, images can be acquired sequentially using the more sensitive LSM 510 channel 1 in multi-track mode. This allows the use of broader filters: long pass filter Lp 475 for CFP and Lp 530 for YFP. Alternatively, and to avoid any cross talk, recover the YFP signal as before and use Bp 470-500 on channel 3 for CFP. These latter parameters will slow the imaging process.

2D or 3D time-lapse:
If maximal capture speed is desired, only one image per time point can be taken, as long as the GFP-spot stays in the imaged plane of focus (called 2D-time-lapse). Often the plane of focus has to be changed manually to follow the spot. Image acquisition in 3D has two main advantages: 1) the GFP-spot does not have to be followed manually as it is always present in one of the focal planes. A subsequent maximal projection along the z-axis produces a complete 2D time sequence without loss of focus on the GFP-spot; 2) After image reconstruction, one can visualise the nucleus and calculate distances in 3D. Such measurements are nonetheless compromised by the reduced optical resolution in z (≥ 0.5 µm for 488nm light).

Specific 3D time-lapse settings are as follows:
6 to 8 optical slices in z, 300-450nm spacing in z with Hyperfine HRZ 200 motor, using a ROI of 3x3-4x4µm, and time intervals of 1.5 seconds. A 12 minute time-lapse series at 0.2% laser transmission did not influence cell cycle progression.

Image Analysis

z-stacks

Determination of the subnuclear position of a GFP tagged locus is monitored relative to the centre of the Nup49-GFP ring. Nuclei in which the tagged locus is at the very top or bottom of the nucleus are not scored, because the pore signal no longer forms a ring but a surface and a peripheral spot will appear internal.

1. Measure the distance from the centre of intensity of the GFP-spot to the nearest pore signal along the nuclear diameter, as well as the nuclear diameter itself, using the middle of the GFP-Nup49 ring as the periphery (Figure 4). Several programs can export coordinates of points of interest, and the publicly available pointpicker plug-in for ImageJ (Rasband) is useful;
2. Calculate the distances/diameter ratio e.g. using Excel. Determine the precise relative radial position by dividing the distance between pore and the spot by half of the calculated diameter, thus normalising distances;
3. Classify each spot's position with respect to three concentric zones of equal surface (Figure 4). The peripheral zone (zone I) is a ring of width=0.184 x the nuclear radius (r). Zone II lies between 0.184r and 0.422r and zone III is the core of the nucleus with radius = 0.578r. The three zones are of equal surface no matter where the nuclear cross-section is taken (see comment 1 and comment 2);
4. Compare the measured distribution to another (e.g. other cell cycle phase, another condition or a random distribution) with a χ^2 analysis. If only percentages of one zone (e.g. the outermost zone) are compared for different conditions (or to a random distribution), a proportional test should be applied. Statistical significance is determined using a 95% confidence interval.

3D-time-lapse

1. Locus tracking: A prerequisite for the precise description of chromatin movement is the knowledge of the coordinates of the locus and of the nuclear centre for each frame of a time-lapse movie. In collaboration with D. Sage and M. Unser (Swiss Federal Institute of Technology, Lausanne) a best fit algorithm has been developed that reliably tracks a moving spot in 2D-time-lapse movies or in maximal projections of z-stacks in 3D-time-lapse using nuclei carrying Nup49-GFP or expressing *tetR*-GFP to detect nucleoplasmic signal. This system is complete and dramatically improves reproducibility and the speed of analysis, while allowing user intervention at several stages. The algorithm has been implemented as a Java plug-in for the public-domain ImageJ software (Rasband; Sage *et al*. 2003). The spatio-temporal trajectory is exported as x,y coordinates for each time point in a spreadsheet. An implementation for 3D image stacks over time will soon be available. Automated image analysis requires three steps:
    a. Alignment phase: The first step is an alignment module that compensates for the translational movement of the nucleus, cell, or microscope stage. This is achieved by a modifiable threshold on the image. The extracted points are then fitted within an ellipse using the least-squares method. Finally, each image is automatically realigned with respect to the centre of the ellipse;
    b. Pre-processing phase: To facilitate the detection of the tagged locus, the images are convolved with a Mexican-hat filter. This pre-processing compensates for background variations and enhances small spot-like structures;
    c. Tracking phase: The final step is the tracking algorithm. Using dynamic programming, which takes advantage of the strong dependency of the spot position in one frame on its position in the next, the optimal trajectory over the entire period of the movie is determined. The following three criteria influence spot recognition: 1. Maximum intensity

(i.e. the tagged DNA is usually brighter than the pore signal); 2. Smoothness of trajectory; 3. Position relative to the nuclear centre. This latter criterion is necessary, because the Nup49-GFP staining can be confused with a weak perinuclear locus. All three parameters can be modulated individually in order to optimise the tracking for different situations (loci that are more mobile, more peripheral, of variable intensity, etc). Most importantly, the program has the option of further constraining the optimisation by forcing the trajectory to pass through a manually defined pixel. In that way mistracked spots can again be added manually to the correct trajectory, which is recalculated quasi-instantaneously. This tracking method proves to be extremely robust and reproducible due to its global approach. Note: Some commercially available software are also able to track objects (e.g. Imaris (Bitplane), Volocity (Improvision)), although tracking efficiency is variable and usually requires uniformly high quality images. The algorithms are mostly based on threshold principles, that are rarely modifiable or interactive.

2. Characterisation of Movement: Because each time lapse series represents a single cell, it is indispensable to average 8-10 movies over a total time > 40 minutes for a given strain or condition. Subtle differences require a larger data source. Useful parameters for quantitative analysis are the following:
    a. Track length: The projected track of the tagged locus can be visualised using the LSM software, ImageJ, Excel or other programs (Figure 5A). The sum of all 1.5 second steps within a time-lapse series yields the total track length of that movie. From this, average track length and velocity (µm/min) can be calculated, but often this parameter is not very revealing;
    b. Step size: Step sizes can be visualized using a box-and-whisker plot. This histogram-like method visualizes the median, the quartiles, the percentiles and the outliers of a distribution. Although being more robust than the track length statistically significant differences are often difficult to detect;
    c. Large movements: Often differences in mobility are not obvious by comparing average speed, yet the frequency of large steps > 500nm will vary significantly. These indicate transient high velocity movements. We generally score for steps larger than 500nm during 7 frames (10.5 seconds), an interval that has proven useful for distinguishing patterns of mobility between different physiological states and stages of the cell cycle (Heun *et al*. 2001b). These are reported as the number of large steps per 10 minutes, averaged over at least 50 minutes of time-lapse imaging. Although a 500nm is a meaningful cut-off, any threshold over 300 nm can be used;
    d. Mean Square Displacement (MSD): Observing the movement of a DNA locus over time does not only give information about its velocity, but also about the subvolume of the nucleus that it occupies during a given period of time. It has been shown for several chromosomal loci that chromosomal domains are able to move apparently randomly in a given sub-volume (Gasser, 2002). This constraint can be quantified by the mean square displacement (MSD) analysis, assuming that the movement of the spot follows a random walk. Ideally it describes a linear relationship between different time intervals and the square of the distance travelled by a particle during this period of time (MSD or $<\Delta d^2>$, where $\Delta d^2 = \{d(t)-d(t+\Delta t)\}^2$ (Berg 1993; Marshall *et al*. 1997; Vazquez *et al*. 2001). In order to get the numbers, one must calculate the distances travelled by the spot for each time interval (1.5s, 3s, 4.5s…) and plot the square of the mean against increasing time intervals. These calculations and the corresponding graphs can be easily performed in Excel (Microsoft) or Mathematica (Wolfram Research). A representative MSD-graph is shown in Figure 5B. In these curves, the slope reflects the diffusion coefficient of the particle, and the linearity of the curve is usually lost at larger time intervals due to spatial constraint on the freedom of movement of the locus. i.e. the particle's random walk is obstructed by the nuclear envelope or other subnuclear constraints, leading to a plateau (horizontal dashed line in Figure 5B). The height of this plateau is related to the volume in which the particle is restricted. The slope of the MSD relation is directly correlated with diffusion coefficient. As explained above, in enclosed systems, diffusion coefficient decreases with increasing µt, due to space constraints exerted on the particle dynamics. Nevertheless, maximal diffusion coefficient can be calculated for very short time intervals and reflects intrinsic mobility of particles (see sloping dashed line in *et al* 5B). For chromosomal loci in yeast we observe maximal diffusion coefficient in the range of $1x10^{-4}$ to $1x10^{-3}\mu m^2/s$, based on short time intervals. If distances are measured between two separate moving loci, <µd2> reflects two times the MSD of an individual spot or locus moving relative to a fixed point (Vazquez *et al*. 2001). A more theoretical discussion of these parameters is found in (Berg 1993).

Materials & Reagents

Yeast minimal and rich media (SD, YPD) are described in Guthrie *et al*. 1991.

Cells can be mounted on a depression slide (Milian SA, Cat. No. CAV-1, Figure 2A) upon 1.4% agarose (Eurobio Cat. No. 018645) containing SD medium with 4% glucose (Fluka). Aliquots of this can be kept at 4°C for several months. Alternatively, cells can be immobilised on a 18mm coverslip treated with Concanavalin A (ConA, Sigma, Cat. No. C-0412) in a cell observation chamber (Ludin chamber, Life Imaging Services, Figure 2B). ConA dissolved to 1mg/ml in H_2O is stable at 20°C for months.

Widefield microscopy is performed on a Metamorph-driven Olympus IX 70 inverted microscope with Olympus Planapo 60x/NA=1.4 or Zeiss Planapo 100x/NA=1.4 objectives on a piezoelectric translator (PIFOC; Physik Instrumente), illuminating with a PolychromeII® monochromator (T.I.L.L. Photonics).

Also needed is a CoolSNAP-HQ Digital camera (Roper Scientific) or equivalent, and both the FITC filter set for detecting GFP (Chroma, Ref. 41001) and the CFP/YFP filter set (e.g.Chroma, Ref. 51017).

Confocal microscopy can be performed on a Zeiss LSM510 Axiovert 200M, equipped with a Zeiss Plan-Apochromat 100x/NA=1.4 oil immersion or a Plan-Fluar 100x/NA=1.45 oil immersion objective. The stage is equipped with a hyperfine motor HRZ 200. Temperature is stabilised using a temperature regulated box surrounding the microscope (The Box, Life Imaging Services).

Software used for analysis is: a) Excel (Microsoft); b) ImageJ public domain software (Rasband); c) Imaris v 3.3 (Bitplane); d) Mathematica 4.1 (Wolfram Research); e). Metamorph v 4.6r6 (Universal Imaging Corp.).

Authors Notes

1. It is very difficult to accurately quantify the intensity of a small, mobile GFP-*lac*^{i} focus. Even in deconvolved images it can differ by 2-fold in sequential images.
2. This protocol shows the optimal method for the described microscope setups. For different microscopes, the values and methods of this protocol are simply a starting point for further optimisation. As improvements in technology (e.g. more sensitive and rapid CCD cameras) and reagents (e.g. more stable or more intense GFP variants) evolve, future adjustments of this protocol will be indispensable.
3. The method described above can also be applied to *Schizosaccharomyces pombe* with a few changes, one being immobilisation on a coverslip with isolectin B (1mg/ml) (Williams *et al*. 2002) or lectin from *Bandeiraea simplicifolia* (Lyophilized powder, Sigma Cat.No. L2380).

Reviewer Comments

Reviewed by: Julio Vazquez, Fred Hutchinson Cancer Research Center, Seattle

1. Perhaps it would be clearer for the readers if the authors gave the radii of regions I, II, and III in figure 4 more explicitly as a function of the radius of the nucleus: if R(I) is the radius of the entire nucleus, then R(II) = 0.816 R(I), and R(III)= 0.578 R(I).
2. When analyzing the data in 3-D, it might be more meaningful to divide the nucleus in three zones of equal volume. In this case, if the radius of the nucleus is R(I), the three shells would have radii equal to R(I), R(II) = 0.87 R(I), R(III)= 0.69 R(I). If spots were to be distributed at random in the nucleus, then the probabilities of finding spots in one of the three shells thus defined would be equal.

   On the other hand, true 3-D measurements are difficult to obtain in microscopy, among other things because of the poorer resolution along the vertical axis. A common practice is to project the data along one axis (generally z), and perform measurements in 2-D. To some extent, this is what happens when imaging single sections of a spherical object (the 2-D image is a projection of a slice defined by the depth of field), and becomes more relevant as the imaged object is small (radius gets closer to the axial resolution of the system), or when the plane of focus gets closer to the poles. In this case, one has to be careful, as none of the radius values given above will partition the image of the nucleus in regions of equal probability. This may not affect conclusions about relative locations of different loci (or the same locus under different conditions), but is clearly important when trying to draw conclusions about whether a given locus is randomly distributed. In this case, simulating a random distribution (as the authors suggest), or consulting with a physicist or mathematician friend for accurate modeling, may be beneficial.

Figures

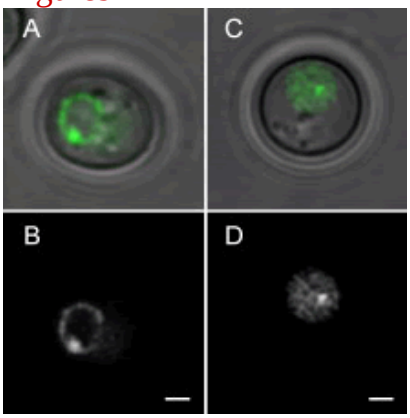

Figure 1. Panel A and C show an overlay of the phase image and the fluorescence image of a GFP tagged yeast cell in G1 phase, panels B and D only the corresponding fluorescence image. The lac^{op} arrays are integrated at the LYS2 locus, the nucleus is visualised by the tagged nuclear pore component Nup49-GFP (A, B) or by using the diffuse staining of nucleoplasm by tetR-GFP (C,D). Bar = 1µm.

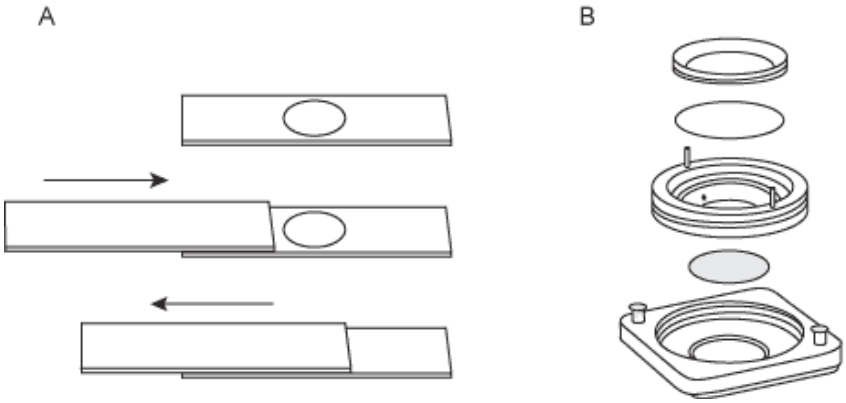

Figure 2. Yeast cells can be immobilised for imaging ether using an agarose patch on a depression slide (A) or using a cell observation chamber (e.g. Ludin chamber; B).

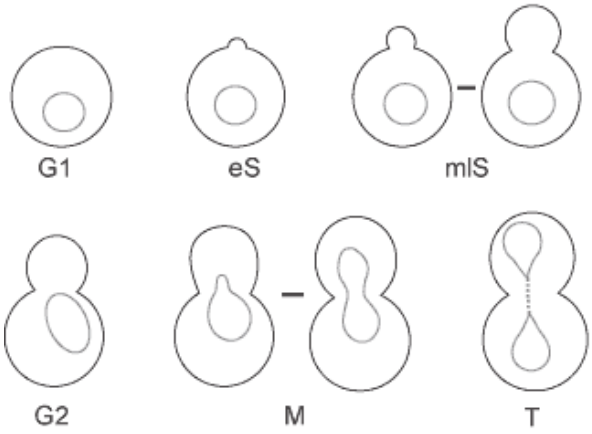

Figure 3. Shown are diagrams of a budding yeast cell at different characteristic points in the cell division cycle. The following criteria are used to identify the indicated stage. G1 phase: unbudded cells with round nuclei, or attached pairs of post-telophase cells that have two round, clearly separated nuclei; early S: with initial bud emergence, cells are in early S; mid-to-late S: cells with a bud big enough to form a ring at the bud neck, in which nuclei are still round and centred in the mother cell; G2 phase: large budded cells (bud ≥ 2/3 of mother) with the nucleus at the bud neck; mitosis (M): large budded cells in which the nucleus extends into the daughter cell due to spindle extension; telophase (T): two globular cells with two distinct nuclei that remain connected by residual NE structures.

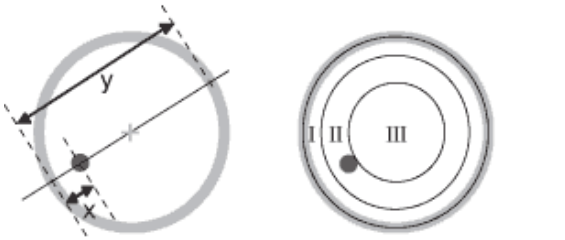

Figure 4. Analysis of DNA locus position. Relative locus position is calculated by normalising measured distance x by the radius (0.5 x measured distance y). The relative radial distances can then be classified and attributed to three groups of equal surface. The peripheral zone (zone I) is a ring of width = 0.184 x the nuclear radius (r). Zone II lies between 0.184r and 0.422r and zone III is the centre of the nucleus with radius=0.578r. In a predicted random distribution every group would contain 1/3 of the cells.

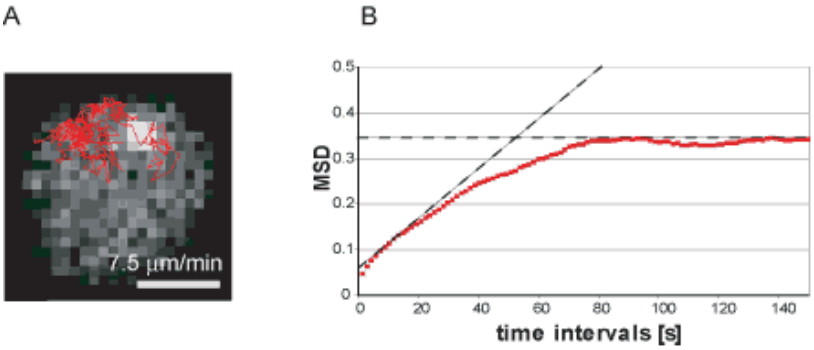

Figure 5. Analysis of DNA locus dynamics. (A) shows the projected trace of 300 images of a movie of the LYS2 locus. The average track length in 5 minutes is 37.4µm. Bar=1µm. (B) shows a mean square displacement (MSD, $<\Delta d^2>$ in [μm^2]) analysis on an average of 8 movies of the LYS2 locus. All cells were observed in G1 phase.

References

1. Belgareh, N. and V. Doye (1997) Dynamics of nuclear pore distribution in nucleoporin mutant yeast cells, *J Cell Biol*, **136(4)**: 747-759.
2. Belmont, A. S. (2001) Visualizing chromosome dynamics with GFP, *Trends Cell Biol*, **11(6)**: 250-257.
3. Berg, H. C. (1993). *Random Walks in Biology*. Princeton University Press, Princeton, New Jersey.
4. Campbell, R. E., O. Tour, A. E. Palmer, P. A. Steinbach, G. S. Baird, D. A. Zacharias and R. Y. Tsien (2002) A monomeric red fluorescent protein, *Proc Natl Acad Sci U S A*, **99(12)**: 7877-7882.
5. Fuchs, J., A. Lorenz and J. Loidl (2002) Chromosome associations in budding yeast caused by integrated tandemly repeated transgenes, *J Cell Sci*, **115(6)**: 1213-1220.
6. Gasser, S. M. (2002) Visualizing chromatin dynamics in interphase nuclei, *Science*, **296(5572)**: 1412-1416.
7. Guthrie, C. and G. R. Fink (1991) *Guide to Yeast Genetics and Molecular Biology*, Academic Press, Inc., San Diego.
8. Hediger, F., F. R. Neumann, G. Van Houwe, K. Dubrana and S. M. Gasser (2002), Live Imaging of Telomeres. yKu and Sir Proteins Define Redundant Telomere-Anchoring Pathways in Yeast, *Curr Biol*, **12(24)**: 2076-2089.
9. Heun, P., T. Laroche, M. K. Raghuraman and S. M. Gasser (2001a) "The positioning and dynamics of origins of replication in the budding yeast nucleus, *Journal of Cell Biology*, **152**: 385-400.
10. Heun, P., T. Laroche, K. Shimada, P. Furrer and S. M. Gasser (2001b) Chromosome dynamics in the yeast interphase nucleus, *Science*, **294(5549)**: 2181-2186.
11. Lisby, M., U. H. Mortensen and R. Rothstein (2003) Colocalization of multiple DNA double-strand breaks at a single Rad52 repair centre, *Nat Cell Biol* **5(6)**: 572-577.
12. Marshall, W. F., A. Straight, J. F. Marko, J. Swedlow, A. Dernburg, A. Belmont, A. W. Murray, D. A. Agard and J. W. Sedat (1997) Interphase chromosomes undergo constrained diffusional motion in living cells, *Current Biology*, **7(12)**: 930-939.
13. Michaelis, C., R. Ciosk and K. Nasmyth (1997) Cohesins: chromosomal proteins that prevent premature separation of sister chromatids, *CellM*, **91(1)**: 35-45.
14. Rasband, W and Image J. Bethesda, Maryland, USA, National Institute of Health.
15. Sage, D., F. Hediger, S. Gasser and M. Unser (2003) Automatic Tracking of Particles in Dynamic Fluorescence Microscopy, *IEEE International Symposium on Image and Signal Processing and Analysis (ISPA 2003)*, Rome, Italy.
16. Straight, A. F., A. S. Belmont, C. C. Robinett and A. W. Murray (1996) GFP tagging of budding yeast chromosomes reveals that protein-protein interactions can mediate sister chromatid cohesion, *Current Biology*, **6(12)**: 1599-1608.
17. Straight, A. F., J. W. Sedat and A. W. Murray (1998) Time-lapse microscopy reveals unique roles for kinesins during anaphase in budding yeast, *J Cell Biol*, **143(3)**: 687-694.
18. Vazquez, J., A. S. Belmont and J. W. Sedat (2001) Multiple regimes of constrained chromosome motion are regulated in the interphase Drosophila nucleus, *Curr Biol*, **11(16)**: 1227-1239.
19. Williams, D. R. and J. R. McIntosh (2002) mcl1+, the Schizosaccharomyces pombe homologue of CTF4, is important for chromosome replication, cohesion, and segregation, *Eukaryot Cell*, **1(5)**: 758-773